Eur. Phys. J. D **16**, 185–188 (2001)

THE EUROPEAN PHYSICAL JOURNAL D

EDP Sciences

Non-collinear magnetic moments of seven-atom Cr, Mn and Fe clusters

N. Fujima[a]

Faculty of Engineering, Shizuoka University, Hamamatsu 432-8561, Japan

Received 30 November 2000

Abstract. The non-collinearity of magnetic moments of pentagonal bipyramid Cr_7, Mn_7 and Fe_7 clusters is discussed. The magnetic moments are calculated by the discrete variational non-collinear spin-density functional method. For the Cr_7 cluster, a coplanar magnetic arrangement appears at the large interatomic distance. With decreasing the interatomic distance, the coplanar arrangement changes to the parallel arrangement with a small absolute magnetic moment. For the Mn_7 cluster, the magnetic arrangement changes from coplanar to antiparallel with decreasing the interatomic distance. Also for the Fe_7 cluster, some coplanar magnetic moments appear at the interatomic distance of 2.23 Å. In these coplanar magnetic arrangements, the magnetic moment at the basal site of the pentagon rotates with a step of 144 degrees for the Cr_7 clusters and 72 degrees for the Mn_7 and Fe_7 clusters.

PACS. 36.40.Cg Electronic and magnetic properties of clusters – 75.75.+a Magnetic properties of nanostructures

1 Introduction

The theoretical study of the non-collinear magnetism has been progressing since the non-collinear spin-density functional calculation was established [1]. The non-collinear spin-density functional method has been applied to the anomalous magnetic system such as metal alloys and metal surfaces [2–5].

In transition metal clusters, especially the mid-3*d* element, Cr, Mn and Fe clusters, the non-collinear magnetism is expected to be observed because the atomic structures of these clusters mainly consist of trigonal or tetrahedral units, where the antiferromagnets are topologically frustrated. However, there have been only a few works in which the non-collinear magnetism is taken into account [6,7]. Oda *et al.* [6] calculated the magnetic moments of structure-optimized Fe_3 and Fe_5 clusters by using the non-collinear local spin-density functional approximation (LSDA) with the ultra soft pseudo potential. They have found that the magnetic moments at the apical sites of the trigonal bipyramid Fe_5 cluster tilt by 30 degrees to those at the basal sites. Ivanov *et al.* [7] have found in their non-collinear wavelet calculation that the directions of magnetic moments in the regular triangle Cr_3 cluster are at 120 degrees with each other on a plane.

In the previous work [8], the author developed a simple method for non-collinear calculation by using the LSDA and the discrete variational (DV) method, and calculated the magnetic moments of 5-atom V, Cr, Mn, Fe, Co, and Ni clusters. The author has found that some coplanar magnetic moments appear in the Cr_5, Mn_5, and Fe_5 clusters. That is, the magnetic moments are ordered not on a line but on a plane in these clusters, whereas only collinear magnetic moments are found in the V_5, Co_5 and Ni_5 clusters.

The method developed in the previous work is so simple that it can be applicable larger system, such as 10-20 atom clusters or surfaces of transition metal. In the present work, we calculate the non-collinear magnetic moments of pentagonal bipyramid Cr_7, Mn_7 and Fe_7 clusters by the non-collinear LSDA-DV method. We find an interesting coplanar magnetic arrangement; magnetic moments rotate along the basal pentagon with a step of ~ 144 degrees for the Cr_7 and ~ 72 degrees for the Mn_7 and Fe_7 clusters.

2 Calculation

All calculations in the present work are performed by the non-collinear LSDA-DV method, which is based on the 2-element non-collinear Kohn-Sham equation [1],

$$\left\{\left(-\nabla^2 + v_0 + \bar{v}_{xc}\right)\boldsymbol{I} + \Delta v_{xc}\tilde{\boldsymbol{\sigma}}_z\right\}\begin{pmatrix}\Psi_i^\alpha\\ \Psi_i^\beta\end{pmatrix} = \varepsilon_i\begin{pmatrix}\Psi_i^\alpha\\ \Psi_i^\beta\end{pmatrix}. \quad (1)$$

Here, $\Psi_i^\sigma(\boldsymbol{r})$ is the one-electron orbital which generates the 2×2 spin-density matrix. v_0 is the electrostatic potential from nuclei and electrons. $\bar{v}_{xc}$ and Δv_{xc} are the

[a] e-mail: fujima@eng.shizuoka.ac.jp

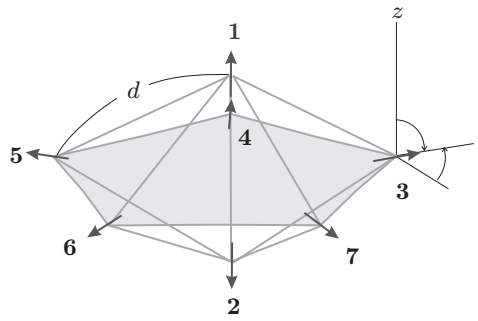

Fig. 1. Atomic structure of pentagonal bipyramid.

spin-independent and the spin-dependent terms of the local exchange correlation potential: $\bar{v}_{xc} = (\delta E_{xc}/\delta\rho^1 + \delta E_{xc}/\delta\rho^2)/2$ and $\Delta v_{xc} = (\delta E_{xc}/\delta\rho^1 - \delta E_{xc}/\delta\rho^2)/2$, where the indices 1, 2 mean the up and down spin along the locally oriented axis. $\delta E_{xc}/\delta\rho^1$ and $\delta E_{xc}/\delta\rho^2$ are obtained by applying the usual LSDA [9] to the spin-densities $\rho^1(\boldsymbol{r})$ and $\rho^2(\boldsymbol{r})$, which are polarized to the local spin-axis at $\boldsymbol{r}$. $\boldsymbol{I}$ is the 2×2 unit matrix, and $\tilde{\boldsymbol{\sigma}}_z$ is the Pauli matrix unitarily transformed by the spin-rotation matrix at each sampling point. Eq. (1) is solved in the self-consistent charge manner with the LCAO basis;

$$\begin{pmatrix} \Psi_k^\alpha \\ \Psi_k^\beta \end{pmatrix} = \sum_i c_{ki} \begin{pmatrix} U_{ki}^1 \\ U_{ki}^2 \end{pmatrix} \phi_i(\boldsymbol{r}), \qquad (2)$$

where c_{ki}, U_{ki}^1 and U_{ki}^2 are complex coefficients. We take numerical bases for the 1s-4s, 2p-4p and 3d atomic orbitals, which are recalculated at every iteration and vary corresponding to the potential around the atom. The calculation is iterated until every charge of atomic orbital converges within the error of 10^{-4}. In this calculation, the relative direction of the magnetic moment at each atomic site is self-consistently obtained. However, the absolute direction cannot be determined. So, in the figures shown below, the direction of the magnetic moment of the atomic site 3 is fixed at $(\theta, \varphi) = (90, 90)$, and the directions for other atoms are shown as the relative angle to it. More details in the method of calculation are described in Ref. [8].

Figure 1 shows the atomic structure of the regular pentagonal bipyramid employed in the present work. The pentagonal pyramid is known as the optimized structure of 7-atom transition metal clusters [10,11]. Instead of optimizing the interatomic distances, we vary the distances from 80% to 100% of those of bulk crystal, and discuss the dependence of the non-collinearity on interatomic distance because the LSDA estimates the interatomic distance shorter than those by experiments or more precise method such as HF-hybrid method, so that the discussion only with the optimized distance would be misleading. Figure 1 also shows the direction of the initial magnetic moment at each atomic site. We take the initial direction from the center to the vertex of the bipyramid. Then, the net initial magnetic moment of the whole cluster is zero. The initial configuration of the 3d electronic states for each atom is taken as follows: $3d_\uparrow^{5.0}3d_\downarrow^{0.0}$ for Cr_5, 4.0, $3d_\uparrow^{5.0}3d_\downarrow^{1.0}$ for Mn_5, and 3.0, $3d_\uparrow^{5.0}3d_\downarrow^{2.0}$ for Fe_5, where the suffix $\uparrow$ ($\downarrow$) means the up (down)-spin about the local axis. The initial configurations of 4s and 4p electronic states are $4s_\uparrow^{0.5}4s_\downarrow^{0.5}4p_\uparrow^{0.0}4p_\downarrow^{0.0}$ for all the clusters.

d/d_{bulk}	Cr	Mn	Fe
1.00	2.23	3.98	2.86
0.95	1.60	3.65	2.86
0.90	0.29	3.21	1.71
0.85	0.29	2.48	1.32
0.80	0.29	0.81	0.29

μ_B/atom

collinear(P) collinear(AP) coplanar non

Fig. 2. Non-collinearity of magnetic moments in the pentagonal bipyramid clusters with the interatomic distance of 80-100% of the bulk value. The magnetic arrangement is indicated by the grayscale. The average magnetic moment per atom (μ_B) is shown for each interatomic distance.

3 Results

3.1 Cr_7

Figure 2 shows the general features of the non-collinearity of the Cr_7 cluster, as well as those of the Mn_7, and Fe_7 clusters with the interatomic distance from 80% to 100% of the bulk value (d/d_{bulk}). In the figure, the magnetic order is shown by the gray scale: parallel (P), antiparallel (AP), coplanar, and non-order. The average absolute magnetic moments per atom (μ_B) are also shown in Fig. 2.

For the Cr_7 cluster, the magnetic moment at each atomic site is arranged in coplanar order for the large interatomic distance. With decreasing the interatomic distance, the absolute magnetic moment per atom rapidly decreases by one tenth and the arrangement changes to the parallel order.

Figure 3 shows the side view of the coplanar magnetic moment of the Cr_7 cluster at the interatomic distance of 2.50 Å ($d/d_{\mathrm{bulk}} = 1.00$). The numbers in the figure correspond to those for the atomic sites in Fig. 1. The direction of the arrow indicates θ in Fig. 1, and the length of the arrow indicates the absolute magnetic moment (μ_B). It is found that the arrow for the basal atomic sites 3-7 rotates clockwise with a similar step of 144 ± 6 degrees. Then, the direction of the magnetic moment rotates twice through the basal pentagon as a kind of the helimagnetic moment.

The magnetic moments at the apical sites 1, 2 is ordered in parallel each other. The absolute value of the magnetic moment is $0.17\mu_B$, which is very small in comparison with those at the basal sites ($\sim 3.0\mu_B$). This is due to the large coordination number at the apical site. It is

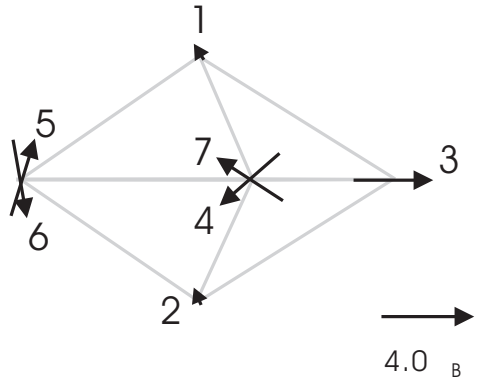

Fig. 3. Side view of the coplanar magnetic moment of the Cr_7 cluster with the interatomic distance of 2.50 Å ($d/d_{\rm bulk} = 1.00$).

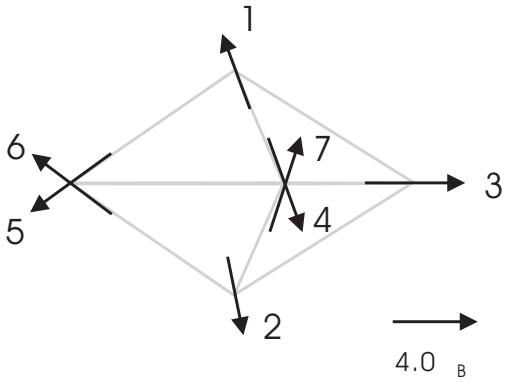

Fig. 4. Side view of the coplanar magnetic moment of the Mn_7 cluster with the interatomic distance of 2.73 Å ($d/d_{\rm bulk} = 1.00$).

known that the magnetic moment for Cr clusters rapidly decreases when the coordination number increases or the interatomic distance decreases [12].

In the small interatomic distance ($d/d_{\rm bulk} = 0.8-0.9$), the magnetic moment at each atomic site aligns in parallel. However, the value of magnetic moment is very small as shown in Fig.2. Total magnetic moment of the whole cluster is $2.0\mu_{\rm B}$, which means that only one electronic level in the majority spin is excessively occupied in comparison with the non-magnetic states.

3.2 Mn_7

Also for the Mn_7 cluster, an almost coplanar magnetic arrangement appears at the large interatomic distance as indicated in Fig. 2. The magnetic arrangement changes from the coplanar to non-coplanar with decreasing the interatomic distance. Finally at 2.18 Å ($d/d_{\rm bulk} = 0.80$), the magnetic moment aligns in antiparallel with a small absolute value ($0.81\mu_{\rm B}$/atom).

Figure 4 shows the same as Fig. 3 for the coplanar magnetic moment of the Mn_7 cluster at the interatomic distance of 2.73 Å ($d/d_{\rm bulk} = 1.00$). The arrow of magnetic moment at the basal sites 3-7 rotates with the step of 72 ± 2 degrees, the half for the Cr_7 cluster. Then, the direction of magnetic moment rotates not twice but once through the pentagon. It is noted that, in this magnetic arrangement, there is a dispersion with ± 5 degrees in the angle from the coplanar plane, whereas the dispersion for the Cr_7 cluster in Fig. 3 is almost zero. Thus, this magnetic arrangement is not complete but almost coplanar and changes to the non-coplanar at smaller interatomic distances.

The magnetic moments at the apical sites align in antiparallel and their absolute values are $3.5\mu_{\rm B}$, which is the five sixth of those of the basal sites. The magnetic arrangement at the apical sites is parallel for Mn_7, while antiparallel for Cr_7 shown in Fig. 3. These arrangements are similar to those for Cr_5 and Mn_5 clusters [8].

Figure 5 shows the non-coplanar magnetic moment of the Mn_7 cluster with the interatomic distance of 2.32 Å

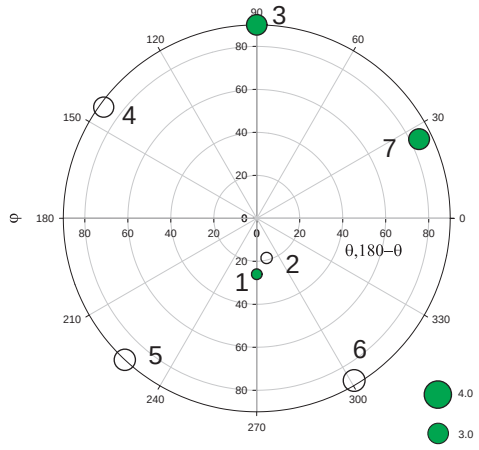

Fig. 5. Polar plot of the non-coplanar magnetic moment of the Mn_7 cluster with the interatomic distance of 2.32 Å ($d/d_{\rm bulk} = 0.85$). The size of symbol indicates the absolute value of the magnetic moment. The radial (azimuthal) part indicates the angle of θ (φ).

($d/d_{\rm bulk} = 0.85$). Here, we employ a polar plot to indicate the direction of the magnetic moment because it is difficult for a 3-dimensional figure to indicate non-coplanar variously oriented magnetic moments with various absolute values. In the figure, the size of symbol indicates the absolute value of the magnetic moment, the filled (empty) symbol means the direction above (below) the horizontal plane. The radius part indicates the angle of θ for $\theta \leq 90$ (above the horizontal plane) or $180 - \theta$ for $90 < \theta \leq 180$ (below the horizontal plane). The azimuthal part indicates the angle of φ.

It is found from Fig. 5 that the magnetic moments orient, in principle, the directions to the center to the vertices of the cluster, that is, those similar to the initial condition. To verify it, we tried some calculation with random initial conditions, and found similar results. We also obtained similar results in the non-coplanar magnetic moments in the Mn_5 cluster [8].

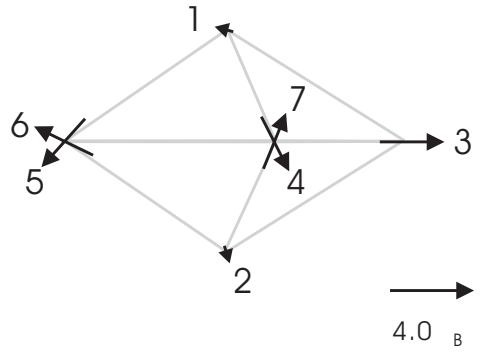

Fig. 6. Side view of the coplanar magnetic moment of the Fe_7 cluster with the interatomic distance of 2.23 Å ($d/d_{\rm bulk} = 0.90$).

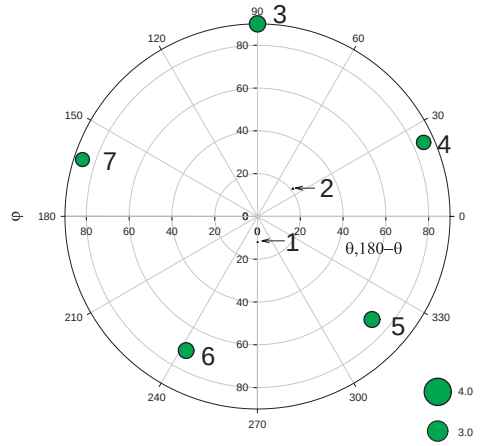

Fig. 7. Polar plot of the non-coplanar magnetic moment of the Fe_7 cluster with the interatomic distance of 2.11 Å ($d/d_{\rm bulk} = 0.85$).

3.3 Fe_7

The magnetic arrangement in the Fe_7 cluster is parallel for large and small interatomic distances as shown in Fig. 2. The absolute magnetic moment decreases from $2.86\mu_{\rm B}$/atom at 2.84 Å ($d/d_{\rm bulk} = 1.00$) to 0.29 at 1.98 Å ($d/d_{\rm bulk} = 0.80$), from 20 to $2\mu_{\rm B}$ in total.

In the intermediate distance, the magnetic arrangement changes to non-collinear. Figure 6 shows the same as Fig. 3 for the coplanar magnetic moment of the Fe_7 cluster with the interatomic distance of 2.23 Å ($d/d_{\rm bulk} = 0.90$). In this arrangement, the dispersion in the angle from the coplanar plane is ±12 degrees. The angle of magnetic moment at the basal sites rotates with the step of 72 ± 12 degrees, so that the magnetic moment rotates once through the vertices of the pentagon similarly to that for the Mn_7 cluster.

The magnetic moments of the apical sites are very small ($0.2\mu_{\rm B}$). These small magnetic moments reduce the average magnetic moment in Fig. 2.

Figure 7 shows the same as Fig. 5 for the non-coplanar magnetic moment of the Fe_7 cluster with the interatomic distance of 2.11 Å ($d/d_{\rm bulk} = 0.85$). The magnetic arrangement is essentially the same as the non-coplanar arrangement for Mn_7 cluster in Fig. 5, that is, the magnetic moments orient to the direction from the center to the vertices of the cluster. It seems that the non-coplanar magnetic arrangements appear around the critical distance where the magnetic moment begins to decrease.

4 Conclusions

The non-collinear magnetic moments of the pentagonal bipyramid clusters, Cr_7, Mn_7, and Fe_7 are calculated by the non-collinear LSDA-DV method. It is found that some coplanar magnetic moments appear in all these clusters. In the coplanar magnetic arrangement, rotating magnetic moments are observed on the basal 5 sites, that is, the magnetic moments rotate with the step of ∼ 144 degrees for the Cr_7 cluster, ∼ 72 degrees for the Mn_7 and Fe_7 clusters.

References

1. J. Kübler, K.-H. Höck, J. Sticht, A.R. Williams, J. Phys. F **18**, 469 (1988).
2. V.P. Antropov, M.I. Katasnelson, M. van Schilfgaarde, B.N. Harmon, Phys. Rev. Lett. **75**, 729 (1995).
3. D. Spišák, J. Hafner, Phys. Rev. B **55**, 8304 (1997).
4. D. Stoeffler, C. Corner, Phil. Mag. B **78**, 623 (1998).
5. L.M. Sandratskii, J. Kübler, Phys. Rev. Lett. **75**, 946 (1995).
6. T. Oda, A. Pasquarello, R. Car, Phys. Rev. Lett. **80**, 3622 (1998).
7. O. Ivanov, V.P. Antropov, J. Appl. Phys. **85**, 4821 (1999).
8. N. Fujima, submitted to Phys. Rev. B.
9. S.H. Vosko, L. Wilk, M. Nusair, Can. J. Phys. **58**, 1200 (1980).
10. P. Ballone, R.O. Jones, Chem. Phys. Lett. **233**, 632 (1994).
11. S. Bouarab, A. Vega, M.J. López, M.P. Iñiguez, J.A. Alonso, Phys. Rev. B **55**, 13279 (1997).
12. K. Lee, J. Callaway, Phys. Rev. B **48**, 15358 (1993).